Characterization of systems of thiophene and benzene with ionic liquids

Marta L.S. Batista, Luciana I.N. Tomé, Catarina M.S.S. Neves, José R.B. Gomes, João A.P. Coutinho *

CICECO, Departamento de Química, Universidade de Aveiro, 3810-193 Aveiro, Portugal

ARTICLE INFO

ABSTRACT

The potential of ionic liquids for aromatic–aliphatic separation or removal of sulfur-containing compounds such as thiophene is well established but, in spite of a number of phase diagrams reported in the literature, the values of other properties required for process design, such as viscosities and densities, are poorly characterized for these mixtures. In this work, systems presenting a LLE with a LCST are studied. Experimental density and viscosity data for binary systems of benzene with $[C_4C_1im][SCN]$, $[C_4C_1im][CF_3SO_3]$ and $[C_2C_1im][NTf_2]$, and thiophene with $[C_4C_1im][SCN]$ and $[C_4C_1im][NTf_2]$ are presented. Additionally, the liquid–liquid phase diagram for the binary system of thiophene with $[C_4C_1im][NTf_2]$ is also reported. The excess molar volumes and viscosity deviations were further estimated and correlated and their values discussed.

© 2013 Elsevier B.V. All rights reserved.

1. Introduction

In the past decades, environmental regulations have become more stringent, requiring the use of more environmentally friendly processes or products. In the petroleum industry, strict regulatory restrictions, requiring the reduction of the level of sulfur and aromatic compound content in fuels to minimize their environmental impact [1,2], have driven the development of new desulfurization processes and of the separation of aromatic and aliphatic hydrocarbons in refineries.

The separation of aromatic and aliphatic hydrocarbons is a challenging task since the conventional distillation process is inefficient due to the close boiling points of these compounds, forming different types of azeotropes. Extractive distillation, azeotropic distillation and liquid–liquid extraction have been used for the removal of those compounds, being the latest the most used technique [3]. Several extractive solvents have been tested for the extraction of toluene, benzene, ethylbenzene or xylene from their mixtures with, for instance, hexane, heptane and octane, but the selection of the solvent to be applied in the extraction processes is still a critical issue [4–7]. For the removal of sulfur compounds, the most common process is hydrodesulfurization (HDS), which uses a catalyst based on CoMo and NiMo working at high temperatures (300–400 °C) and pressures (20–100 bar of H_2) [2]. This technology has proved to be very efficient for the removal of aliphatic sulfur compounds (thiols, thiolethers and disulfides), but was found to be ineffective for aromatics such as thiophene, benzothiophene, dibenzothiophene and their alkyl derivatives [8]. Moreover, to achieve very low sulfur levels, HDS requires more severe operational conditions which imply high costs but also have the disadvantage of saturating olefins, which are important for fuel performance [8]. Oxidative desulfurization, reactive adsorption, biodesulfurization, membranes, extractive desulfurization and the particularly promising liquid–liquid extraction have been proposed as alternative processes [8–12].

The selection of the extraction solvent is a crucial step since it affects the efficiency of the separation. Until recently, conventional organic compounds, such as sulfolane, were typically used as extraction solvents, but environmental issues and the additional operation costs associated to their regeneration have led to the search for convenient alternatives [1]. Due to their unique properties, ionic liquids (ILs) have been identified as advantageous substitutes for VOCs in separation processes, among various other applications [1,3]. Composed of a large asymmetric organic cation and an organic or inorganic anion, ILs are characterized by low melting points, a wide range of liquidus state, high thermal and chemical stability, densities higher than common organic solvents, low solubility in aliphatic hydrocarbons and high solubility in aromatic compounds (and consequently high selectivity in the separation of aromatics from aliphatic compounds). Furthermore, they have negligible vapor pressure, and their recovery is easy requiring fewer operational steps and low energy consumption, offering additionally the possibility of tuning their properties by changing the cation or the anion that composes the IL, to meet the requirements of the envisaged process [3,13–15].

In order to properly design the separation processes and choose the most suitable IL to perform the extraction, the knowledge of the thermophysical properties of ILs, including density and viscosity, as well as the liquid–liquid equilibrium (LLE) phase diagrams of their binary and ternary mixtures with aromatic compounds, is required [16,17]. Studies devoted to the separation of aromatic from aliphatic compounds using ILs composed by different combinations of cations (imidazolium, pyridinium, pyrrolidinium, ammonium or phosphonium)

---

* Corresponding author. Tel.: +351 234 370200; fax: +351 234 370084.
E-mail address: jcoutinho@ua.pt (J.A.P. Coutinho).

and anions (hexafluorophosphate, tetrafluoroborate, thiocyanate, dicyanamide, bis[(trifluoromethyl)sulfonyl]imide) have been extensively reported and reviewed by Ferreira et al. [13,14]. These reviews provide a very complete compilation of LLE data for binary and ternary systems involving ILs, and aromatic and aliphatic hydrocarbons. Additionally, several studies on the application of ILs for the removal of sulfur compounds have also been reported in the literature and a large number of ILs including imidazolium [18–20], pyridinium [21,22], Lewis and Brönsted acid and oxidative ILs [23,24] have been tested as extractive solvents. Anions such as bis[(trifluoromethyl)sulfonyl]imide, hexafluorophosphate, tetrafluoroborate, ethylsulfate, acetate and thiocyanate have been considered, with the latest showing higher selectivity [2,25–27]. While measuring the binary [16,25,26,28,29] and ternary [1,2,9,12] phase diagrams of systems composed of sulfur compounds and ILs, different LLE behaviors were observed for systems of ILs and thiophene, depending on the IL anion. In most cases, these systems show the common upper critical solution temperature (UCST) with their mutual miscibilities increasing with temperature, for example, 1-butyl-3-methylimidazolium bis[(trifluoromethyl)sulfonyl]imide with thiophene, but some systems display a lower critical solution temperature (LCST), for instance, 1-butyl-3-methylimidazolium thiocyanate with thiophene and benzene. These systems are the object of characterization in this work.

Herein, the densities and viscosities of the binary systems of [C_4C_1im][SCN] with thiophene, and of [C_4C_1im][SCN], [C_4C_1im][CF_3SO_3] and [C_2C_1im][NTf_2] with benzene, were measured at atmospheric pressure and in the temperature range from 298.15 to 328.15 K. The thermophysical properties and phase diagram of the binary system composed of [C_4C_1im][NTf_2] with thiophene was also measured since it was not previously reported in the open literature and it was relevant for this work for comparison purposes. Excess molar volumes and viscosity deviations were additionally estimated and correlated by the Redlich–Kister polynomial expansion.

2. Experimental

2.1. Materials

Thiophene was supplied by Acros with a purity of 99.5 wt.% and benzene by Merck with a purity of 99.7 wt.%. The ILs used in this work were supplied by IoLiTec and comprise 1-butyl-3-methylimidazolium bis(trifluoromethylsulfonyl)imide, [C_4C_1im][NTf_2], mass fraction purity >99 wt.%, 1-butyl-3-methylimidazolium thiocyanate, [C_4C_1im][SCN], mass fraction purity >98 wt.%, 1-butyl-3-methylimidazolium triflate, [C_4C_1im][CF_3SO_3], mass fraction purity >99 wt.%, and 1-ethyl-3-methylimidazolium bis(trifluoromethylsulfonyl)imide, [C_2C_1im][NTf_2], mass fraction purity >99 wt.%. Their purities were further confirmed by ^{1}H, ^{13}C and ^{19}F (whenever applicable) NMR. In order to reduce the amount of volatile impurities, all samples were dried for at least 48 h under vacuum (10^{-5} Pa) at room temperature before use. After the drying procedure, the water content in the samples range from 208 to 324 ppm, measured by Karl–Fischer titration. The molecular structures of the compounds studied in this work are presented in Fig. A.1 (Appendix A - Supplementary data).

2.2. Experimental procedure

Mixtures of thiophene with [C_4C_1im][SCN] and [C_4C_1im][NTf_2], as well mixtures of benzene with [C_4C_1im][SCN], [C_4C_1im][CF_3SO_3] and [C_2C_1im][NTf_2] were prepared gravimetrically with an uncertainty of ±10^{-5} g. In order to homogenize the mixtures, they were constantly stirred for at least 24 h at room temperature.

2.2.1. Density and viscosity

Density and viscosity measurements were performed at atmospheric pressure and in the temperature range from 283.15 to 333.15 K, using an automated SVM 3000 Anton Paar rotational Stabinger viscometer–

densimeter. The SVM 3000 Anton Paar rotational Stabinger viscometer–densimeter uses Peltier elements for fast and efficient thermostatization. This equipment has been previously tested and used by us [30–32] for density and viscosity measurements of ionic liquids and ionic liquid systems. The uncertainty in temperature is within ±0.02 K. The relative uncertainty for the dynamic viscosity is ±0.35% and the absolute uncertainty for density is ±0.5 kg m^{-3}.

2.2.2. Liquid–liquid equilibrium

The phase diagram for the binary system of thiophene and [C_4C_1im][NTf_2] was measured by turbidimetry. The onset of the liquid–liquid immiscibility (cloud point temperature) was determined by visual observation of the phase demixing (turbidity followed by phase separation). Mixtures were introduced in Pyrex-glass capillaries with a stirrer, and the concentration range studied, $0.15 < x_{IL} < 0.17$, was restricted by experimental limitations (the visual method was not applicable at mole fractions of the IL out of this range, since the experimental setup is limited either for low or high temperatures) and was established on the basis of titrations carried out prior to the experiments. The sealed capillaries were placed in a thermostated bath and were kept under continuous stirring during the whole experiment. Solutions presenting two phases at ambient temperature were heated into the homogeneous region and then slowly cooled until visual detection of phase demixing. The cooling rate was about 10 °C for each 30 min. The temperature at which the first sign of turbidity appeared upon cooling was taken as the temperature of the liquid–liquid phase transition. For monophasic solutions at room temperature, the heating process was suppressed. The temperature was controlled with a calibrated U1252A, Handheld Digital Multimeter 4.5-digit associated to a calibrated Pt100 temperature sensor immersed in the thermostating liquid. This equipment has an uncertainty of ±0.01 K. Three consistent measurements were carried out for each solution.

2.3. Thermodynamic models—mixture properties

The excess thermodynamic properties are employed to describe the deviation in behavior of a mixture from the ideality, giving important information concerning the nature of the molecular interactions present in binary systems. The excess molar volumes, V^E, were estimated from the measured densities according to the following equation,

$$V^E = \sum x_i M_i \left(\frac{1}{\rho_{mixt}} - \frac{1}{\rho_i} \right) \tag{1}$$

where x_i, M_i, and ρ_i are, respectively, the molar fraction, molar mass, and density for each component of the binary system, and ρ_{mixt} is the density of the mixture.

Similarly, viscosity deviations were estimated from measured viscosities according to the following equation,

$$\Delta \ln(\eta) = \ln(\eta_{mixt}) - \sum x_i \ln(\eta_i) \tag{2}$$

where x_i and η_i are, respectively, the molar fraction and viscosity for each component that composes the binary system, and η_{mixt} is the viscosity of the mixture.

The excess volumes and viscosity deviations were correlated at each temperature with a Redlich–Kister polynomial expansion as shown in the following equation,

$$Q = x_{aromatic} x_{IL} \sum_{j=0}^{m} A_j (x_{aromatic} - x_{IL})^j \tag{3}$$

where Q represents either the excess molar volume V^E, or the viscosity deviations $\Delta \eta$, $x_{aromatic}$ corresponds to the molar fraction of benzene or thiophene, x_{IL} is the molar fraction for all ILs studied, A_j are the correlation parameters, and m is the degree of the polynomial expansion. For

our systems, a second-order polynomial was found to be an adequate level for V^E, and a first-order polynomial for $\Delta\eta$.

3. Results and discussion

3.1. Liquid–liquid equilibrium (LLE)

Fig. 1 shows the liquid–liquid phase diagram measured in this work for the binary system of thiophene and $[C_4C_1im][NTf_2]$ (the experimental data is supplied as Supplementary data, Table A.1), along with the liquid–liquid phase diagrams of mixtures of $[C_4C_1im][SCN]$, and $[C_4C_1im][CF_3SO_3]$ with thiophene, taken from literature [25,26]. Two distinct types of phase behavior are observed, with ($[C_4C_1im][NTf_2]$ + thiophene) presenting the UCST-type of liquid–liquid phase diagram and the two other systems displaying LCST behavior.

3.2. Densities and viscosities (ρ, η)

The experimental data for the density, ρ, and viscosity, η, obtained in this work are compiled in Tables 1 and 2. For all the systems studied, the density presents a linear dependence with temperature, whereas the viscosity presents the expected exponential dependence, in the entire range of compositions. The values of both properties decrease with the increase of temperature and aromatic compound concentration, with the pure IL presenting the highest values for these properties (Appendix A - Supplementary data—Figs. A.2, A.3 and A.5). The exception is the system of thiophene with $[C_4C_1im][SCN]$, for which the density decreases with an increase of IL concentration. In the latter case, densities of the mixtures are higher than that of the pure IL (Fig. A.4 at Appendix A - Supplementary data).

3.3. Excess molar volumes (V^E) and viscosity deviations ($\Delta\eta$)

The estimated excess molar volumes, V^E, and viscosity deviations, $\Delta\ln(\eta)$, of the binary systems composed by the ILs and benzene or ILs and thiophene are depicted in Figs. 2 to 5. The corresponding data are provided as Supplementary data (Tables A.2 and A.3). The Redlich–Kister coefficients obtained in the estimation of V^E and $\Delta\ln(\eta)$ are compiled in Tables 3 and 4. In general, the Redlich–Kister polynomial expansion correlates successfully the data of V^E and $\Delta\ln(\eta)$, providing a good description of the solution behavior of all the binary systems studied.
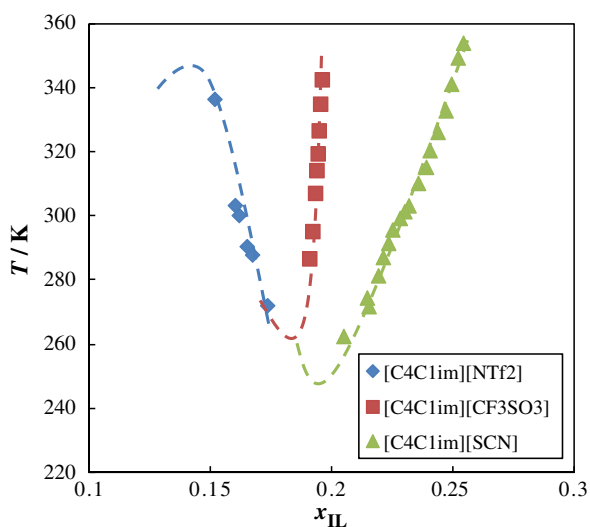

Fig. 1. Liquid–liquid phase diagrams for $[C_4C_1im][NTf_2]$ (measured in this work), $[C_4C_1im][SCN]$ [25] and $[C_4C_1im][CF_3SO_3]$ [26] with thiophene. Dashed lines are guides to the eye.

Table 1
Experimental density as a function of temperature for pure ionic liquids, thiophene, benzene and for their mixtures, in different mole fractions and at atmospheric pressure.

$[C_4C_1im][SCN]$ + thiophene			
		T/K	
x_{IL}	298.15	308.15	318.15	328.15
		ρ/g cm^{-3a}	
1.000	1.070	1.064	1.058	1.052
0.897	1.073	1.067	1.061	1.055
0.857	1.075	1.068	1.062	1.056
0.754	1.077	1.070	1.064	1.058
0.390	1.082	1.075	1.068	1.061
0.299	1.084	1.076	1.069	1.061
0.000	1.059	1.047	1.034	1.022
$[C_4C_1im][NTf_2]$ + thiophene			
		T/K	
x_{IL}	298.15	308.15	318.15	328.15
		ρ/g cm^{-3}	
1.000	1.437	1.428	1.418	1.409
0.911	1.429	1.420	1.410	1.401
0.724	1.406	1.396	1.386	1.376
0.664	1.397	1.387	1.377	1.368
0.439	1.369	1.359	1.349	1.339
0.230	1.308	1.298	1.287	1.277
0.000	1.059	1.047	1.034	1.022
$[C_4C_1im][SCN]$ + benzene			
		T/K	
x_{IL}	298.15	308.15	318.15	328.15
		ρ/g cm^{-3}	
1.0000	1.072	1.066	1.060	1.054
0.7666	1.053	1.046	1.040	1.034
0.7420	1.050	1.044	1.038	1.031
0.6081	1.036	1.029	1.023	1.017
0.4906	1.019	1.012	1.005	0.999
0.0000	0.874	0.863	0.852	0.841
$[C_4C_1im][CF_3SO_3]$ + benzene			
		T/K	
x_{IL}	298.15	308.15	318.15	328.15
		ρ/g cm^{-3}	
1.000	1.300	1.292	1.284	1.276
0.878	1.280	1.272	1.264	1.256
0.696	1.246	1.237	1.229	1.221
0.647	1.232	1.224	1.216	1.208
0.427	1.169	1.160	1.152	1.143
0.000	0.874	0.863	0.852	0.841
$[C_2C_1im][NTf_2]$ + benzene			
		T/K	
x_{IL}	298.15	308.15	318.15	328.15
		ρ/g cm^{-3}	
1.000	1.519	1.509	1.499	1.489
0.865	1.490	1.480	1.469	1.460
0.661	1.431	1.421	1.411	1.401
0.529	1.381	1.371	1.360	1.350
0.508	1.373	1.363	1.352	1.342
0.000	0.874	0.863	0.852	0.841

[a] Standard uncertainties u are $u(T) = 0.02$ K, $u(p) = 10$ kPa, and the combined expanded uncertainty U_c is $U_c(\rho) = 0.5$ kg m^{-3}, with an expanded uncertainty at the 0.95 confidence level (k ~ 2).

Negative excess molar volumes are observed for all the mixtures considered, in the entire range of composition. The same temperature dependence – a decrease of V^E with the increase of temperature – is also observed for all the systems, as shown in Fig. 2 for mixtures of $[C_4C_1im][SCN]$ with benzene. The negative values of V^E are indicative of favorable interactions between both aromatic compounds and the ILs. Differences in the magnitude of V^E values can be related to several effects, such as the size and structure of the species and the type/strength of the interactions present in the mixture. The first effect influences the effective packing of the solute/solvent molecules, hindering or promoting specific and oriented interactions, while the type or strength of the interactions depends on the nature of the compounds.

Both benzene and thiophene possess an aromatic ring with delocalized π-electrons, being thus able to establish π–π interactions

Table 2
Experimental viscosity data as function of temperature for pure ionic liquids, thiophene, and benzene, and also for their mixtures, in different mole fractions and at atmospheric pressure.

x_{IL}	298.15	308.15	318.15	328.15
$[C_4C_1im][SCN]$ + thiophene T/K				
		η/mPa s[a]		
1.000	57.396	37.358	25.801	18.697
0.897	47.236	31.408	22.072	16.222
0.857	42.880	28.748	20.364	15.071
0.754	31.952	22.025	15.962	12.024
0.390	13.355	9.937	7.672	6.103
0.299	9.926	7.566	5.959	4.834
0.000	0.655	0.585	0.525	0.470
$[C_4C_1im][NTf_2]$ + thiophene T/K				
		η/mPa s		
1.000	51.320	34.434	24.353	17.981
0.911	42.625	29.035	20.805	15.528
0.724	26.615	18.817	13.903	10.658
0.664	23.223	16.584	12.367	9.545
0.439	14.725	10.949	8.449	6.721
0.230	6.861	5.347	4.288	3.525
0.000	0.655	0.585	0.525	0.470
$[C_4C_1im][SCN]$ + benzene T/K				
	η/mPa s			
1.0000	62.810	40.562	27.836	20.086
0.7666	32.980	22.508	16.197	12.192
0.7420	30.691	21.072	15.231	11.518
0.6081	20.092	14.292	10.641	8.250
0.4906	12.511	9.269	7.157	5.650
0.0000	0.605	0.527	0.466	0.363
$[C_4C_1im][CF_3SO_3]$ + benzene T/K				
		η/mPa s		
1.000	87.964	56.429	38.308	27.254
0.878	64.295	42.193	29.228	21.168
0.696	37.168	25.406	18.233	13.621
0.647	32.799	22.579	16.331	12.299
0.533	19.811	14.218	10.644	8.200
0.427	12.622	9.370	7.215	5.715
0.000	0.605	0.527	0.466	0.363
$[C_2C_1im][NTf_2]$ + benzene T/K				
		η/mPa s		
1.000	33.001	23.663	17.693	13.679
0.865	25.188	18.438	14.017	10.930
0.661	15.638	11.755	9.107	7.258
0.529	11.405	8.654	6.803	5.503
0.508	10.402	7.979	6.314	5.159
0.000	0.605	0.527	0.466	0.363

[a] Standard uncertainties u are $u(T) = 0.02$ K, $u(p) = 10$ kPa, and the combined expanded uncertainty U_c is $U_c(\eta) = 0.35\%$, with an expanded uncertainty at the 0.95 confidence level ($k \sim 2$).
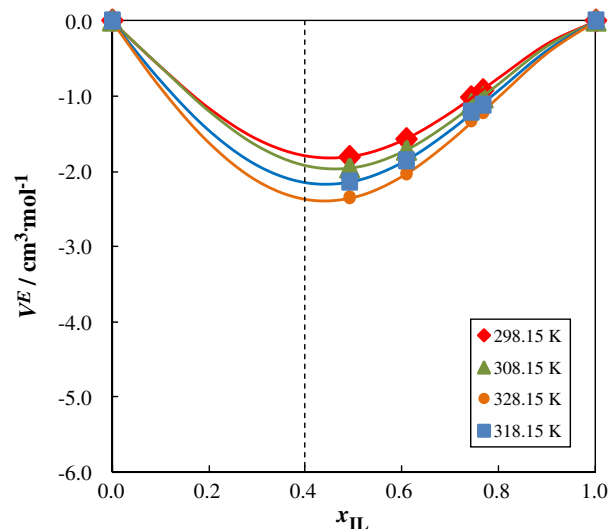

Fig. 2. Excess molar volumes as a function of the mole fraction of the IL, in mixtures of $[C_4C_1im][SCN]$ with benzene, at different temperatures, namely, (♦) 298.15 K, (▲) 308.15 K, (■) 318.15 K and (●) 328.15 K. Solid lines represent the corresponding correlation of Redlich–Kister. The dotted line corresponds to the limit of miscibility, where at the left is the immiscibility region.

with the imidazolium cation of the IL. However, the lone electron pairs on the sulfur atom of thiophene confer a higher polarity to this molecule, and consequently stronger interactions with the IL ions are likely to take place.

The benzene-containing systems present negative values of V^E in the entire range of compositions, and they are very similar to each other, having the maximum V^E values ranging from −2.35 to −2.85 cm³ mol⁻¹, for $[C_4C_1im][SCN]$ and $[C_4C_1im][CF_3SO_3]$, respectively. Consistently, larger negative V^E values are observed for the thiophene-containing systems. The $[C_4C_1im][NTf_2]$–thiophene mixtures present negative values of V^E which are larger than the values obtained for $[C_4C_1im][SCN]$. That system also shows a different concentration dependency than all the other systems studied, with a minimum at lower concentrations. Its V^E values are also less dependent with temperature. The different behavior of this system suggests that it is ruled by a different type of interactions, which is in agreement with the observed differences in the phase diagram behavior.

As illustrated in Fig. 4 for the $[C_4C_1im][SCN]$–thiophene mixtures, the values obtained for the $\Delta \ln(\eta)$ are positive and decrease with temperature for all the systems studied, in the entire range of compositions. As shown in Fig. 5, two different behaviors are observed for the viscosity deviations. Smaller values of $\Delta \ln(\eta)$ are found for the benzene-containing mixtures, while the thiophene systems present larger values of $\Delta \ln(\eta)$. This pattern can be related to the polarity of the aromatic compound, which is higher in the case of thiophene, leading to stronger interactions with the ILs. Slightly lower viscosity deviations are observed for the $[SCN]^-$-containing systems, suggesting that the dominant effect is the possibility to establish more points of contact, which is more likely in the cases of $[C_2C_1im][NTf_2]$, $[C_4C_1im][NTf_2]$ and $[C_4C_1im][CF_3SO_3]$, than in the case of $[C_4C_1im][SCN]$.
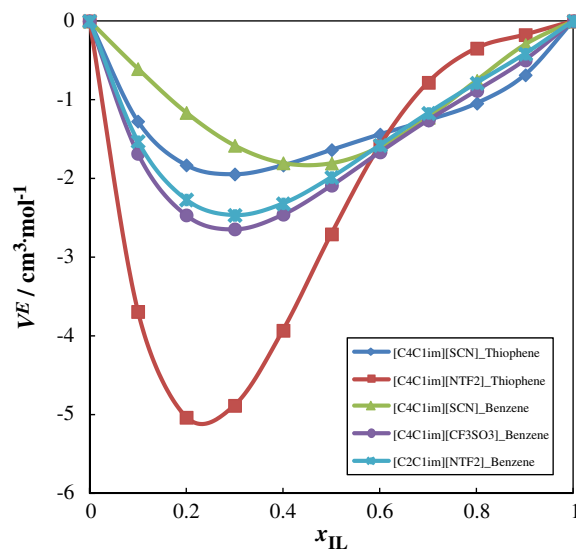

Fig. 3. Estimated excess molar volumes through Redlich–Kister's correlation as a function of the mole fraction of the IL, at 298.15 K.
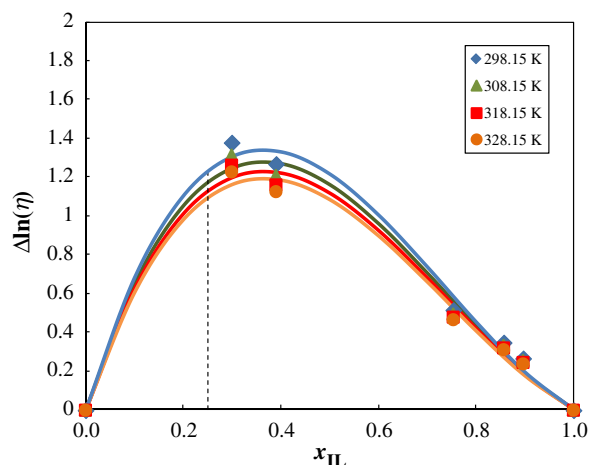
Fig. 4. Viscosity deviations as a function of the mole fraction of the IL, in mixtures of [C$_4$C$_1$im][SCN] with thiophene, at different temperatures, namely, (◆) 298.15 K, (▲) 308.15 K, (■) 318.15 K and (●) 328.15 K. Solid lines represent the corresponding correlation of Redlich–Kister. The dotted line corresponds to the limit of miscibility, where at the left is the immiscibility region.

4. Conclusions

In this work, experimental density and viscosity data are reported for systems of benzene with [C$_4$C$_1$im][SCN], [C$_4$C$_1$im][CF$_3$SO$_3$] and [C$_2$C$_1$im][NTf$_2$], and for systems of thiophene with [C$_4$C$_1$im][SCN] and [C$_4$C$_1$im][NTf$_2$]. The experimental liquid–liquid equilibrium phase diagram for the binary system of thiophene with [C$_4$C$_1$im][NTf$_2$] is also reported. The experimental densities and viscosities were used to estimate the excess molar volumes and the viscosity deviations of the mixtures. These data were successfully correlated with the Redlich–Kister polynomial expansion, providing a good description of the solution behavior of the studied systems.

The results obtained show a decrease of the density and of the viscosity with temperature and with the increase of benzene or thiophene content in the mixture, with the pure ILs presenting the highest values. A distinct behavior is found for the system of thiophene with [C$_4$C$_1$im][SCN], for which the density decreases with the increase of x_{IL}. All the mixtures studied show negative values of V^E and positive $\Delta\ln(\eta)$, in all ranges of compositions. Factors such as the size, structure and nature

of the compounds present in the mixtures, and the consequent type and strength of the interactions established were considered to explain the behavior of the solutions. A different behavior is observed for the [C$_4$C$_1$im][NTf$_2$]–thiophene mixtures, with larger values of V^E and with a different concentration dependency than for all the other systems studied, that correlates well with the observed differences in the phase diagram behavior.

Acknowledgements

Table 3
Coefficients for Redlich–Kister correlations for excess molar volume.

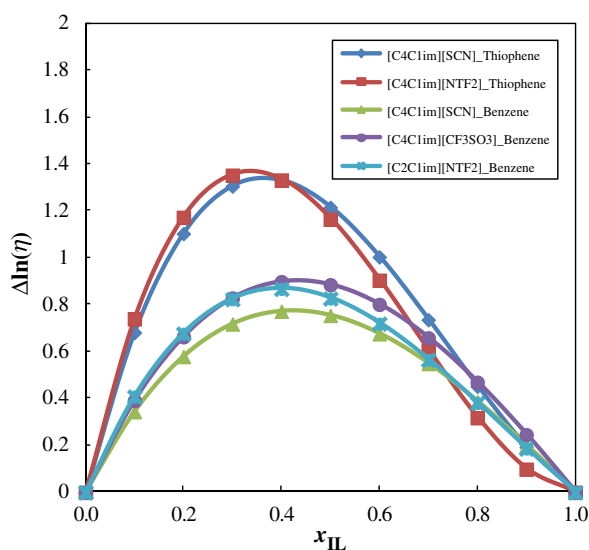|	T/K			
	[C$_4$C$_1$im][SCN] + thiophene			
RK coeff	298.15	308.15	318.15	328.15
A$_o$	−6.541	−7.155	−7.814	−8.660
A$_1$	−4.087	−4.815	−5.515	−6.269
A$_2$	−6.778	−7.327	−7.872	−8.309
	[C$_4$C$_1$im][NTf$_2$] + thiophene			
RK coeff	298.15	308.15	318.15	328.15
A$_o$	−10.825	−11.213	−11.704	−12.321
A$_1$	−24.428	−25.217	−25.910	−26.835
A$_2$	−16.642	−17.145	−17.670	−18.293
	[C$_4$C$_1$im][SCN] + benzene			
RK coeff	298.15	308.15	318.15	328.15
A$_o$	−7.225	−7.794	−8.528	−9.358
A$_1$	−2.122	−1.887	−2.789	−3.175
A$_2$	3.414	4.073	3.117	3.303
	[C$_4$C$_1$im][CF$_3$SO$_3$] + benzene			
RK coeff	298.15	308.15	318.15	328.15
A$_o$	−8.349	−8.851	−9.498	−10.119
A$_1$	−8.242	−8.515	−8.990	−9.463
A$_2$	−5.867	−5.692	−5.870	−6.146
	[C$_2$C$_1$im][NTf$_2$] + benzene			
RK coeff	298.15	308.15	318.15	328.15
A$_o$	−7.937	−8.412	−8.936	−9.459
A$_1$	−7.716	−8.003	−7.921	−8.242
A$_2$	−4.485	−4.626	−4.079	−4.645

Fig. 5. Estimated viscosity deviations through Redlich–Kister's correlation as a function of the mole fraction of the IL, at 298.15 K.

Table 4
Coefficients for Redlich–Kister correlations for viscosity deviations.

	T/K			
	[C$_4$C$_1$im][SCN] + thiophene			
RK coeff	298.15	308.15	318.15	328.15
A$_o$	4.862	4.639	4.458	4.331
A$_1$	3.391	3.219	3.078	2.990
	[C$_4$C$_1$im][NTf$_2$] + thiophene			
RK coeff	298.15	308.15	318.15	328.15
A$_o$	4.660	4.424	4.234	4.100
A$_1$	4.452	4.217	4.025	3.896
	[C$_4$C$_1$im][SCN] + benzene			
RK coeff	298.15	308.15	318.15	328.15
A$_o$	3.017	2.948	2.894	3.095
A$_1$	1.004	1.041	1.080	1.202
	[C$_4$C$_1$im][CF$_3$SO$_3$] + benzene			
RK coeff	298.15	308.15	318.15	328.15
A$_o$	3.542	3.411	3.301	3.480
A$_1$	1.010	1.053	1.080	1.285
	[C$_2$C$_1$im][NTf$_2$] + benzene			
RK coeff	298.15	308.15	318.15	328.15
A$_o$	3.306	3.175	2.957	3.253
A$_1$	1.541	1.420	1.731	1.542

Appendix A. Supplementary data

Figures containing density and viscosity, as function of temperature, for [C4C1im][CF3SO3] with benzene and [C4C1im][SCN] with thiophene; tables containing excess molar volume and viscosity deviations data; liquid–liquid equilibrium data measured in this work. Supplementary data to this article can be found online at http://dx.doi.org/10.1016/j.molliq.2013.10.014.

References

[1] A. Arce, M.J. Earle, H. Rodriguez, K.R. Seddon, A. Soto, Green Chem. 10 (2008) 1294–1300.
[2] K. Kedra-Krolik, M. Fabrice, J.-N. Jaubert, Ind. Eng. Chem. Res. 50 (2011) 2296–2306.
[3] G.W. Meindersma, A.R. Hansmeier, A.B. de Haan, Ind. Eng. Chem. Res. 49 (2010) 7530–7540.
[4] S.H. Ali, H.M.S. Lababidi, S.Q. Merchant, M.A. Fahim, Fluid Phase Equilib. 214 (2003) 25–38.
[5] R. Krishna, A.N. Goswami, S.M. Nanoti, B.S. Rawat, M.K. Khanna, J. Dobhal, Indian J. Technol. 25 (1987) 602–606.
[6] J. Mahmoudi, M.N. Lotfollahi, J. Chem. Thermodyn. 42 (2010) 466–471.
[7] Y. Yorulmaz, F. Karpuzcu, Chem. Eng. Res. Des. 63 (1985) 184–190.
[8] A.R. Hansmeier, G.W. Meindersma, A.B. de Haan, Green Chem. 13 (2011) 1907–1913.
[9] M. Francisco, A. Arce, A. Soto, Fluid Phase Equilib. 294 (2010) 39–48.
[10] R. Anantharaj, T. Banerjee, Fuel Process. Technol. 92 (2011) 39–52.
[11] P.S. Kulkarni, C.A.M. Afonso, Green Chem. 12 (2010) 1139–1149.
[12] K. Kedra-Krolik, F. Mutelet, J.-C. Moise, J.-N. Jaubert, Energy Fuel 25 (2011) 1559–1565.
[13] A.R. Ferreira, M.G. Freire, J.C. Ribeiro, F.M. Lopes, J.G. Crespo, J.A.P. Coutinho, Ind. Eng. Chem. Res. 50 (2011) 5279–5294.
[14] A.R. Ferreira, M.G. Freire, J.C. Ribeiro, F.M. Lopes, J.G. Crespo, J.A.P. Coutinho, Ind. Eng. Chem. Res. 51 (2012) 3483–3507.
[15] G.W. Meindersma, A. Podt, M.B. Klaren, A.B. De Haan, Chem. Eng. Commun. 193 (2006) 1384–1396.
[16] U. Domanska, M. Zawadzki, M.M. Tshibangu, D. Ramjugernath, T.M. Letcher, J. Chem. Thermodyn. 42 (2010) 1180–1186.
[17] M. Krolikowska, M. Karpinska, M. Zawadzki, J. Phys. Chem. B 116 (2012) 4292–4299.
[18] L. Alonso, A. Arce, M. Francisco, O. Rodriguez, A. Soto, AlChE J. 53 (2007) 3108–3115.
[19] Y. Mochizuki, K. Sugawara, Energy Fuel 22 (2008) 3303–3307.
[20] Y. Nie, C. Li, A. Sun, H. Meng, Z. Wang, Energy Fuel 20 (2006) 2083–2087.
[21] H. Gao, M. Luo, J. Xing, Y. Wu, Y. Li, W. Li, Q. Liu, H. Liu, Ind. Eng. Chem. Res. 47 (2008) 8384–8388.
[22] J.D. Holbrey, I. Lopez-Martin, G. Rothenberg, K.R. Seddon, G. Silvero, X. Zheng, Green Chem. 10 (2008) 87–92.
[23] A. Bosmann, L. Datsevich, A. Jess, A. Lauter, C. Schmitz, P. Wasserscheid, Chem. Commun. 23 (2001) 2494–2495.
[24] N.H. Ko, J.S. Lee, E.S. Huh, H. Lee, K.D. Jung, H.S. Kim, M. Cheong, Energy Fuel 22 (2008) 1687–1690.
[25] U. Domańska, M. Krolikowski, K. Slesinska, J. Chem. Thermodyn. 41 (2009) 1303–1311.
[26] A. Marciniak, E. Karczemna, Fluid Phase Equilib. 307 (2011) 160–165.
[27] A.L. Revelli, F. Mutelet, J.N. Jaubert, J. Phys. Chem. B 114 (2010) 4600–4608.
[28] U. Domanska, M. Krolikowski, J. Chem. Thermodyn. 42 (2010) 355–362.
[29] J. Lachwa, J. Szydlowski, A. Makowska, K.R. Seddon, J. Esperanca, H.J.R. Guedes, L.P.N. Rebelo, Green Chem. 8 (2006) 262–267.
[30] C.M.S.S. Neves, M.L.S. Batista, A.F.M. Claudio, L.M.N.B.F. Santos, I.M. Marrucho, M.G. Freire, J.A.P. Coutinho, J. Chem. Eng. Data 55 (2010) 5065–5073.
[31] C.M.S.S. Neves, P.J. Carvalho, M.G. Freire, J.A.P. Coutinho, J. Chem. Thermodyn. 43 (2011) 948–957.
[32] A. Bhattacharjee, C. Varanda, M.G. Freire, S. Matted, L.M.N.B.F. Santos, I.M. Marrucho, J.A.P. Coutinho, J. Chem. Eng. Data 57 (2012) 3473–3482.